Chebyshev approximations for an inhomogeneously broadened line-shape in Mössbauer spectroscopy

H. Flores Llamas
Instituto Nacional de Investigaciones Nucleares
Mártires de la Conquista y Carlos B. Zetina, Col. Escandón, Delegación M. Hidalgo
Apartado postal 18-1027, 11801 México, D.F., Mexico

Recibido el 19 de junio de 1997; aceptado el 20 de mayo de 1998

We present the analysis of an inhomogeneously broadened Mössbauer line-shape, from which we obtained a power series expansion, that includes the absorber thickness (T_a) and the interference effects (ξ_0). At the same time, we give the area and depth dependency formulae as function of the T_a and ξ_0 parameters. A new line-shape is built as a lineal combination of the traditional transmission integral (TI) with the inhomogeneously broadened line-shape, which is useful for absorbers that have a partial or total inhomogeneous broadening. Finally, a comparative analysis of the obtained results for the potassium ferrocyanide compound and the stainless steel foil is carried out using the new line-shape with respect to the TI to show its reliability.

Keywords: Chebyshev polynomials; Mössbauer spectroscopy; line-shape and absorber thickness parameter

Presentamos el análisis de una forma de línea Mössbauer ensanchada inhomogéneamente, llegando a una expansión en serie de potencias que incluye el grueso del absorbedor (T_a) y los efectos de interferencia (ξ_0). Asimismo, presentamos fórmulas de la dependencia del área y la profundidad como función de los parámetros T_a y ξ_0. Una nueva forma de línea es construida a partir de una combinación lineal de la integral de transmisión (IT) tradicional con la forma de línea ensanchada inhomogéneamente, la cual es útil para absorbedores que tienen un ensanchamiento inhomogéneo parcial o total. Una comparación de los resultados obtenidos para el compuesto de ferrocianuro de potasio y una lámina de acero inoxidable, usando la nueva forma de línea con respecto a IT, es llevada a cabo mostrando su confiabilidad.

Descriptores: Polinomios de Chebyshev; espectroccopía Mössbauer; forma de línea y parámetro del grueso del absorbedor

PACS: 76.80

1. Introduction

A widely treated topic since the beginning of the Mössbauer spectroscopy has been the line-shape of the observed spectrum [1–12]. The line-shape routinely analyzed has been represented by the so called transmission integral (TI), which assumes a cross-section of Lorentzian line-shapes in the emission and absorption [1–3, 5–9, 11, 13–26]. The model represented by the TI has been used successfully, since specific information about the dependence of the recoilless fraction on temperature has been obtained for experimental spectra analyzed with the TI [13, 27]. However, the spectroscopists who have used the TI have not been able to analyze some line-shapes, such as those coming from substances that present a broadening due to a distribution of its hyperfine parameters [28–32]. Due to the anomalous line-shapes present in alternative experimental spectra, models like the one represented by the TI have been proposed.

An alternative model for the line-shape has been suggested by several authors [7, 33, 34]; this model contains the TI as a particular case when there is no selfabsortion in the source. This line-shape is obtained by the substitution of the Lorentzians (emission and absorption cross-sections) from the TI by Voigt line-shapes. In this model, that can be called Voigt transmission integral (VTI), only its full width has been analyzed numerically as a function of the thickness parameter T_a [34]. The Voigt line-shape contains the Lorentzian and Gaussian line-shapes as limit cases [35], and experimental evidence of this line-shapes has been reported in the source [36] and in the absorber [32].

A particular case of the VTI model was used formerly by Margulies *et al.* [6], for the stainless steel spectrum, which is not adjustable by the TI. These authors obtained several experimental spectra using a source and an absorber of stainless steel. The spectra were analyzed with the IT, and with an alternative line-shape obtained from the substitution of the Lorentzians by Gaussians, in the emission and absorption cross-sections of the IT. For this latter line-shape, Margulies *et al.* calculated an exact analytical expansion. They analyzed the widths of the line-shape as functions of the thickness parameter T_a using the TI and its alternative line-shape, and at last they found, for each one of the two methods, different results. Therefore, they concluded that "when dealing with broadened Mössbauer lines, analysis based on simple spectral shape must be applied with discrimination" [6].

Another particular case of the VTI, analyzed by Lang [7] and O'Connor and Skyrme [33], consists of a Lorentzian emission and a Voigt absorption line-shapes. This model is

more realistic than the one analyzed by Margulies *et al.*, since the emission line-shape for thin sources is represented by the Lorentzian line-shape more ordinarily than by a Gaussian one. This model has been scarcely used due to the lack of a power series expansion that allows to evaluate its line-shape. The analysis of this line-shape has been exiguous, its area [7, 33] and width [7] parameters have only been numerically calculated as functions of T_a.

In the Sect. 2 of this paper a power series expansion for a particular VTI case, which considers a Lorentzian emission and a Gaussian absorption, is presented. A Gaussian absorption is referred to an absorber with an inhomogeneous completely broadened line-shape. Lang calculated analytically only the area [7] for this line-shape. In the present analysis the interference parameter (ξ_0) [37] is also included, for which experimental and theoretical values have been given for different Mössbauer isotopes [38, 39]. In the Sect. 3, a new line-shape for Mössbauer spectroscopy is expressed as a lineal combination of the former line-shape with the TI. This new line-shape is useful in the analysis of absorbers with an inhomogeneous broadening as it will be seen.

2. Analytical calculation of the completely inhomogeneous case

Considering Lorentzian emission and Gaussian absorption with an interference parameter ξ_0, the transmission line-shape for a single line in Mössbauer spectroscopy, is given by

$$n_G(v,T_a) = \frac{2f_s n_0}{\Gamma_s \pi}\int_{-\infty}^{+\infty}\frac{(\Gamma_s/2)^2\,dE}{(\Gamma_s/2)^2+(E-v)^2} \times \exp\left\{-T_a\left(\frac{\Gamma_a/2-2\xi_0 E}{\Gamma_a/2}\right) \times \exp\left[-\left(\frac{E}{\Gamma_a/(2\sqrt{\ln 2})}\right)^2\right]\right\} + (1-f_s)n_0 + n_a, \quad (1)$$

where E is the integration variable (mm/s), v the source velocity, n_G (v,T_a) the number of counts observed at each velocity v in the spectrum, $T_a = \sigma_0 f_a t_a d$ the effective absorber thickness, t_a the number of Mössbauer atoms per unit area in the absorber, d the fraction of abundance of the Mössbauer isotope, σ_0 the absorption cross-section, f_s, f_a the source and absorption recoilless fractions, Γ_s, Γ_a emission and absorption full widths at half maximum (fwhm), n_0 the number of gamma rays of the Mössbauer transition, and $n_a$the number of additional counts due to other transitions,

With the following substitutions in Eq. (1): $N = n_a + n_0(1-f_s)$, $M = n_0 f_s$, $w_s = \Gamma_s/2$ and $w_a = \Gamma_a/2$, this expression can be rewritten as

$$n_G(V,T_a) = \frac{M}{\pi}\int_{-\infty}^{+\infty}\frac{w_s\,dE}{w_s^2+(E-v)^2} \times \exp\left\{-T_a\left(\frac{w_a-2\xi_0 E}{w_a}\right) \times \exp\left[-\left(\frac{E}{w_a\sqrt{\ln 2}}\right)^2\right]\right\} + N \quad (2)$$

To calculate the above expression, first the exponential function in the integral is developed as a series of Chebyshev polynomials [40]:

$$\exp\{-T_a G_a(E)\} = \exp\left(-\frac{T_a}{2}\right) \times \left[I_0\left(\frac{T_a}{2}\right) + 2\sum_{n=1}^{\infty}(-1)^n I_n\left(\frac{T_a}{2}\right)T_n^*[G_a(E)]\right] \quad (3)$$

where T_n^* are the shifted Chebyshev polynomials, I_n are the modified Bessel functions, and

$$G_a(E) = \left(\frac{w_a-2\xi_0 E}{w_a}\right)\exp\left[-\left(\frac{E}{w_a/\sqrt{\ln 2}}\right)^2\right].$$

Equation (3) is only valid when $0 \le G_a(E) \le 1$. It is easy to demonstrate that when $\xi_0 \ll 1$, (the order of our approximation) the inequality is fulfilled. Substituting Eq.(3) into Eq. (1) and rearranging the result, the following equation is obtained:

$$n_G(v,T_a) = M\exp(-T_a/2) \times \left[D_0(T_a/2) + \sum_{n=1}^{\infty} D_n(T_a/2)P_n(v)\right] + N, \quad (4)$$

where the D_n and P_n are defined by
i) $D_0(T_a/2) = I_0(T_a/2) + 2\sum_{n=1}^{\infty} I_n(T_a/2) = \exp(T_a/2)$;
ii) $D_n(T_a/2)$ are sums of binary products from shifted Chebyshev polynomials coefficients (b_{nk}) and from $2(-1)^n I_n(T_a/2)$. A general method for calculating the D_n is not feasible, since there is not any closed analytic relation to calculate the coefficients b_{nk}. Using the coefficients b_{nk} given in Luke's book [41], and the similar form employed in Appendix A of Ref. 26, we calculate the first twelve D_n coefficients listed in Table I.
iii) The $P_n(v)$ integrals in Eq. (4) are given by

$$P_n(v) = \frac{1}{\pi}\int_{-\infty}^{+\infty}\frac{w_s\,dE}{w_s^2+(E-v)^2}\left(\frac{w_a-2\xi_0 E}{w_a}\right)^n \times \exp\left[-\left(\frac{E}{w_a/\sqrt{\ln 2}}\right)^2 n\right]. \quad (5)$$

To calculate the $P_n(v)$, we transform Eq. (5) by substituting $y_n = E\sqrt{n\ln 2}/w_a$ into Eq. (5), obtaining

$$P_n(a,v) = \frac{a}{\pi}\int_{-\infty}^{+\infty}\frac{(1-2\xi y_n)^n\exp(-y_n^2)}{a^2+(u-y_n)^2}\,dy_n, \quad (6)$$

TABLE I. Coefficients for expansion of the D_n polynomials $D_n(T_a/2) = 2\sum_{k=n}^{m}(-1)^n b_{n,k} I_k(T_a/2)$, where m is the order of the approximation, for example, if $m = 4$ then: $D_1 = 2(-2I_1 - 8I_2 - 18I_3 - 32I_4)$; $D_2 = 2(8I_2 + 48I_3 + 160I_4)$; $D_3 = 2(-32I_3 - 256I_4)$; $D_4 = 2(128I_4)$.

n	b_{n1}	b_{n2}	b_{n3}	b_{n4}	b_{n5}	b_{n6}	b_{n7}	b_{n8}	b_{n9}	b_{n10}	b_{n11}	b_{n12}
1	2	8	18	32	50	72	98	128	162	200	242	288
2		8	48	160	400	840	1568	2688	4320	6600	9680	13728
3			32	256	1120	3584	9408	21504	44352	84480	151008	256256
4				128	1280	6912	26880	84480	228096	549120	1208064	2471040
5					512	6144	39420	180224	658944	2050040	5637632	14057472
6						2048	28672	212992	1118208	4659200	16400384	50692096
7							8192	131072	1105920	6553600	30638080	120324096
8								32768	589824	5570560	36765696	190513152
9									131072	2621440	27394048	199229440
10										524288	11534336	132120576
11											20927152	50331648
12												8388608

where $a = (w_s/w_a)\sqrt{n\ln 2}$, $\xi = \xi_0/\sqrt{n\ln 2}$ and $u = \sqrt{n\ln 2}/w_a v$ (a, ξ, and u are successions of n and they should carry subindex n, but n has been omitted in order to avoid making the notation confusing). Nevertheless, its dependency should be kept in mind in the remaining calculations. Developing the numerator of the integral in Eq. (6) to terms of order ξ^2, we have

$$P_n(a,u) = P_{n1}(a,u) - 2n\xi P_{n2}(a,u) + 2n(n-1)\xi^2 P_{n3}(a,u), \quad (7)$$

where:

$$P_{n1}(a,u) = \frac{a}{\pi}\int_{-\infty}^{+\infty} \frac{\exp(-y_n^2)}{a^2+(u-y_n)^2}\,dy_n, \quad (8)$$

$$P_{n2}(a,u) = \frac{a}{\pi}\int_{-\infty}^{+\infty} \frac{y_n\exp(-y_n^2)}{a^2+(u-y_n)^2}\,dy_n, \quad (9)$$

$$P_{n3}(a,u) = \frac{a}{\pi}\int_{-\infty}^{+\infty} \frac{y_n^2\exp(-y_n^2)}{a^2+(u-y_n)^2}\,dy_n. \quad (10)$$

Equation (8) is the Voigt line-shape, which in our context represents a Lorentzian line-shape source of half-width $w_s\sqrt{n}$ and a Gaussian line-shape absorber of half-width w_a. The ratio "a" determines the proportionality between the Lorentzian and the Gaussian characteristics of the line-shape, so that if $a = 0$, Eq. (8) is reduced to a pure Gaussian, but if $a = \infty$ a pure Lorentzian is obtained, as it has been shown by Elste [42]. If $\Gamma_s(= 2w_s)$ and $\Gamma_a(= 2w_a)$ are taken equal to the natural width Γ_0, then the ratio "a" is reduced to

$$a = \frac{w_s}{w_a}\sqrt{n\ln 2} = \sqrt{n\ln 2}.$$

The minimum value of "a" occurs when $n = 1$, which corresponds to $a = \sqrt{\ln 2}$. Using the derivatives of the Voigt line-shape [43] one can easily show that the integral (9) and (10) are given by

$$P_{n2}(a,u) = uP_{n1}(a,u) - aK(a,u), \quad (11)$$

$$P_{n3}(a,u) = \left[u^2 - a^2\right]P_{n1}(a,u) - 2auK(a,u) + a/\sqrt{\pi}, \quad (12)$$

where $K(a,u)$ is defined by

$$K(a,u) = \frac{1}{\pi}\int_{-\infty}^{+\infty}\frac{(u-y)\exp(-y^2)}{a^2+(u-y)^2}\,dy$$

If P_{n1}, P_{n2}, and P_{n3}, given by Eqs. (8), (11) and (12) are substituted into Eq. (7), and if $P_n(a,v)$ thus obtained is substituted into Eq. (4), then we obtain the following power series:

$$n_G(v,T_a) = M\Big\{1 + \exp(-T_a/2)\sum_{n=1}^{\infty} D_n(T_a/2) \times \Big(P_{n1} + 2n\xi(uP_{n1} - aK) + 2n(n-1)\xi^2 \times \left[(u^2-a^2)P_{n1} - 2auK + a/\sqrt{\pi}\right]\Big)\Big\} + N, \quad (13)$$

where a, u, and ξ as defined in Eq. (6). The dependency on "a" and u of $P(a,u)$ and $K(a,u)$ has been omitted. Equation (13) represents the Mössbauer line-shape of a Lorentzian source without self absorption, with a Gaussian absorber and the interference effect. Equation (13) can be used as a trial function in a standard least squares fitting to an experimental spectrum. For the case where $\xi = 0$, Eq. (13) becomes

$$n_G(v,T_a) = M\Big[1 + \exp(-T_a/2) \times \sum_{n=1}^{\infty} D_n(T_a/2)P_{n1}(a,u)\Big] + N. \quad (14)$$

For the case when $T \ll 1$, Eq. (14) becomes

$$n_G(v,T_a) = M\left[1 - T_a P_{n1}(a,u)\right] + N, \quad (15)$$

since $I_n(T_a/2) = (T_a/4)^n/\Gamma(n+1)$ [44], where $a = (w_s/w_a)\sqrt{\ln 2}$, $u = (\sqrt{\ln 2}/w_a)v$. Equation (15)

represents a Voigt line-shape which does not have the same physical meaning as the Voigt line-shape presented by Kobayashi and Fukumura [34] for $T_a \ll 1$. In their case, the Gaussian full width represents the source and absorber inhomogeneities, and the Lorentzian full width represents the sum of the source and absorber widths. In our case, the Gaussian width is the full width of the absorber, and the Lorentzian width is the full width of the source.

2.1. Depth and area

2.1.1. Depth

The depth D for $w_s \neq w_a$ defined by $v = 0$ in Eq. (13) coincides with the maximum depth only for $\xi = 0$. The expression for D is as follows:

$$D = -M \exp(-T_a/2) \sum_{n=1}^{\infty} D_n(T_a/2) \times \left[P_{n1}(a,0) + 2n\xi + 2n(n-1)\xi^2 \times \left(-a^2 P_{n1}(a,0) + a/\sqrt{\pi}\right)\right], \quad (16)$$

since $K(a,0) = 0$ [43], where $P_{n1}(a,0) = \exp(a^2)\,\mathrm{erfc}\,(a)$, and $\mathrm{erfc}\,(a)$ is the error function complementary.

2.1.2. Area

The area A for $w_s \neq w_a$ is obtained by direct integration of the summation in Eq. (13) in the following form:

$$A = -M \exp(-T_a/2) \sum_{n=1}^{\infty} D_n(T_a/2) \times \int_{-\infty}^{+\infty} \left\{P_{n1} - 2n\xi\left(uP_{n1} - aK\right) + 2n(n-1)\xi^2\left[(u^2 - a^2)P_{n1} - 2auK + a/\sqrt{\pi}\right]\right\} dv. \quad (17)$$

To calculate the above integral, it is first integrated with respect to y_n and after with respect to v, obtaining the following result:

$$A = -M \exp(-T_a/2) w_a \sqrt{\frac{\pi}{\ln 2}} \times \sum_{n=1}^{\infty} \frac{D_n(T_a/2)}{\sqrt{n}} \left[1 + \frac{n(n-1)}{\ln 2}\xi_0^2\right],$$

where ξ has been substituted for its value $\xi = \xi_0/\sqrt{n \ln 2}$.

2.2. Numerical calculation of $n_G(v, T_a)$

Figure 1a shows Eq. (14) calculated to an order $m = 12$, and $T_a = 15$, $M = w_s = 1$, $N = 0$, $w_a = 2$ and $\xi_0 = 0$. The line-shape calculated with Eq. (14) is very similar to the one

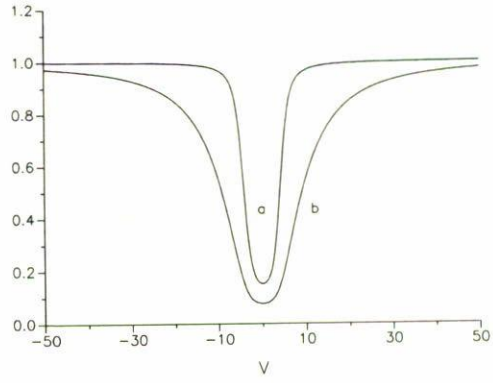

FIGURE 1. (a) Eq. (14) calculated to an order of $m = 12$ and $T_a = 15$, $M = 1$, $w_s = 1$, $N = 0$, $\xi_0 = 0$, and $w_a = 2$. (b) integral transmission calculated with the same parameters values of (a) as given in Fig. 1 of Ref. 26. The area and depth parameters of the line-shape with absorption Lorentzian are greater than those corresponding to the absorption Gaussian.

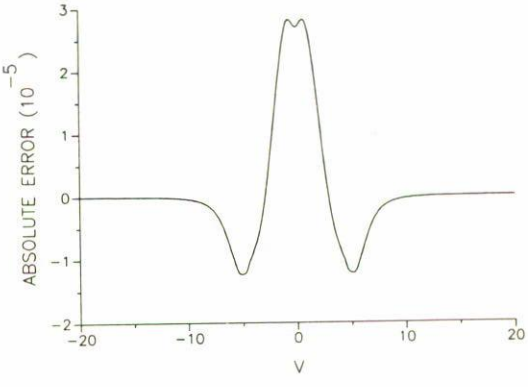

FIGURE 2. Absolute error (simple differences) between Eqs. (1) and (14) for the spectrum shown in Fig 1a

simulated with Eq. (1) as it can be seen in Fig. 2, where the absolute error is shown. The absolute error of Eq. (14) with respect to Eq. (1), in the cases of $T_a < 15$, is lower than that shown in Fig. 2; for example, the case $T_a = 4$, $w_a = 2w_s = 2$ and $\xi_0 = 0$ presents a maximum error of less than 0.17 ppm for the order of $m = 10$, as shown in Fig. 3c. To analyze the approximation of Eq. (13) to the interference term, the difference $n_G(T_a = 4,\ \xi_0 = 0.01) - n_G(T_a = 4,\ \xi_0 = 0)$ was calculated directly from Eq. (1) and was compared with the terms that involve ξ_0 in Eq. (13) with $m = 12$. The maximum absolute error between both calculations was of 0.7 ppm, as shown in Fig. 4. From the comparison of Fig. 3c ($m = 10$) and Fig. 4 ($m = 12$) it can be seen that the greater contribution to the error of Eq. (13) is given by the corresponding terms of the interference parameter. Thus, to reduce this error in Eq. (13) ξ-terms of higher order m with respect to the order of the no ξ-terms should be taken. To calculate the well known functions $P(a,u)$ and $K(a,u)$ involved in $n_G(v,T_a)$, we used the approximation of Gautschi's to the complex error function $W(u,\hat{\imath}a)$ [45]. The relationships among $W(u,\hat{\imath}a)$, $P_{n1}(a,u)$ and $K(a,u)$ are given in Ref. 46.

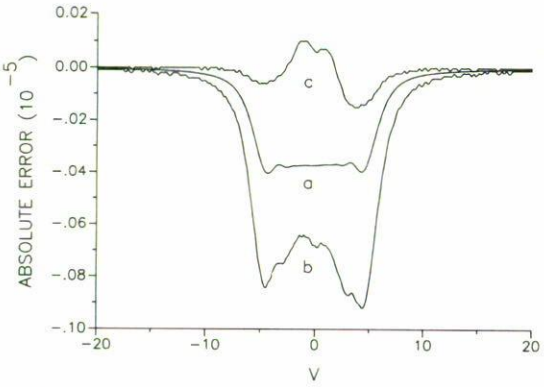

FIGURE 3. Absolute error (simple differences) between Eqs. (1) and (14) with $T_a = 4$, $w_a = 2w_s = 2$, $\xi_0 = 0$, $N = 0$ and $M = 1$ for the order: (a) $m = 8$, (b) $m = 9$, (c) $m = 10$. Curve (a) was multiplied by the amount of 0.05. This change is due for convenience of displaying.

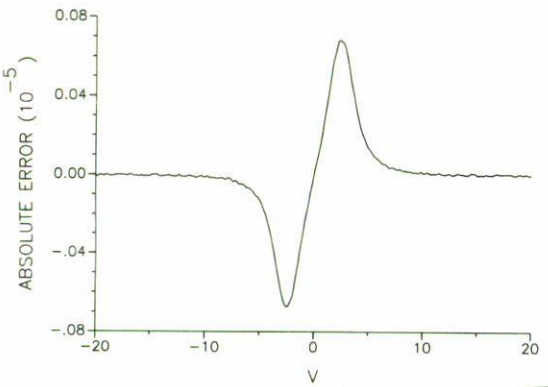

FIGURE 4. Absolute error between $n_G(T_a = 4,\ \xi_0 = 0.01) - n_G(T_a = 4,\ \xi_0 = 0)$ and Eq. (13) for only the terms containing $\xi_0 (= 0.01)$.

3. Lineal Combination

From the observation of the curves 1a and 1b in Fig. 1, it is suggested that the line-shape of a spectrum that presents a Lorentzian-Gaussian mixture in the absorber could be approximated through a lineal combination of the curves 1a and 1b as follows:

$$n_I(v, T_a) = k n_e(v, T_a) + (1 - k) n_G(v, T_a), \qquad (18)$$

where $n_G(v, T_a)$ is defined by Eq. (14) and $n_e(v, T_a)$ is the transmission integral given by [26]

$$n_e(v, T_a) = M\Big\{1 + \exp(-T_a/2) w_a' \times \sum_{n=1}^{\infty} 2 I_n(T_a/2) \mathrm{Im}[\mathbb{Z}_n(z)]\Big\} + N, \qquad (19)$$

where w_a' is the Lorentzian half-width of the absorber, I_n are the modified Bessel functions, all the other parameters $(M, T_a, v, w_s$ and $N)$ are taken equal as in Eq. (14), and $\mathbb{Z}_n(z)$ are the generalized Lorentzian functions and are defined in Ref. 26:

$$\mathbb{Z}_n(z) = 2 \begin{cases} \dfrac{\sum_{k=0}^{(n-1)/2} \binom{n}{2k} z^{2k} (\hat{\imath} w_a')^{n-2k-1}}{(z + \hat{\imath} w_a')^n}, & \text{if } n \text{ is odd}, \\ \dfrac{\sum_{k=0}^{(n-2)/2} \binom{n}{2k+1} z^{2k+1} (\hat{\imath} w_a')^{n-2(k+1)}}{(z + \hat{\imath} w_a')^n}, & \text{if } n \text{ is even}, \end{cases} \qquad (20)$$

where $z = v + \hat{\imath} w_s$. Equation (18) is similar to that employed as an approximation for the Voigt line-shape [47, 48], where the $2w_a'$ (Lorentzian) and $2w_a$ (Gaussian) widths are taken equal, and in principle different from $2w_s$. Equation (18) is only valid for the case of $\xi = 0$, since Eq. (19) is only valid for this case. The k parameter in Eq. (18) is the absorber Lorentzian-Gaussian fraction, and its value is restricted between 0 and 1; it is obvious that when $k = 1$ or $k = 0$ the TI case or the completely inhomogeneous case are recovered.

3.1. Experimental applications

We now want to show Eq. (18) in two practical examples, in which their spectra cannot be fitted by the TI, since a strong inhomogeneous broadening is present. Equation (18) will show its utility in the case where T_a and $w_a' = w_a$ parameters are unknown. Both spectra were accumulated with a source of 20 mCi of Co^{57} diffused into Rodhium with a width of 0.1 mm/s [49], and a maximum velocity of 3.0 ± 0.008 mm/s determined by the laser interferometric method. The gamma ray counts were stored in 256 channels. The background counts due to high energy gamma ray were measured by the method described in Ref. 50. Experimental spectra of potassium ferrocyanide compound and stainless steel foil at room temperature were fitted with Eq. (18). The best fitting is shown in Figs. 5 and 6 with a solid line (—) and experimental data are shown with dots (···). As it can be seen, there is a good agreement between the fitting curve and the experimental points. The retrieved Mössbauer parameters obtained from the fittings with Eqs. (14), (18) and (19) to the experimental data, are listed in Table II. The source width Γ_s was fixed in all the fittings to the value 0.1 mm/s.

If we compare the T_a parameters obtained by the lineal combination Eq. (18) with that obtained by TI, it can be seen that TI gives wrong fits with a larger χ^2. From our analysis for the potassium ferrocyanide, $T_a = 0.83$ and the absorber Mössbauer fraction f_a is 0.292, for a value of the cross section of $\sigma_0 = 2.35 \times 10^{-18}$ cm^2. The obtained value of f_a is the arithmetic average of the values obtained by Ball and Lyle [51] $f_a = 0.281$, and Kobayashi and Fukumura [34]

TABLE II. Results of fitting procedures applied to two samples.

Parameter	potassium ferrocyanide			stainless steel		
	Eq. (14)	Eq. (18)	Eq. (19)	Eq. (14)	Eq. (18)	Eq. (19)
k	—	0.603	—	—	0.367	—
T_a	0.706	0.830	0.779	1.55	1.790	2.71
$2w_a^{(a)}$ (mm/s)	0.121	0.0976	0.1[b]	0.186	0.167	0.107
centre (mm/s)	−0.138	−0.139	−0.139	−0.190	−0.190	−0.190
depth (counts)	296050	314519	306882	24349	25580	27745
baseline (counts)	3912040	3919862	3926016	131081	131953	132679
$\chi^{2(c)}$	1788	546	1897	400	215	559

[a] The fwhm is $\Gamma_a = 2w_a$.

[b] Value anomalously small of w_a was obtained when w_a was left to converge freely, then its inferior limit of convergence was fixed at 0.05 mm/s.

[c] The fitting quality is calculated through the quantity $\sum$ (experimental value-fitted value)^2 /(experimental value).

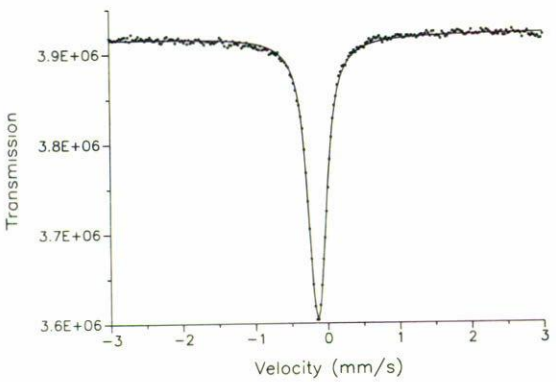

FIGURE 5. Fitting result with Eq. (18), calculated for $n = 8$ terms, for the spectrum of $K_4Fe(CN)_6 3H_2O$ compound with a thickness of 5.0 mg/cm^2.

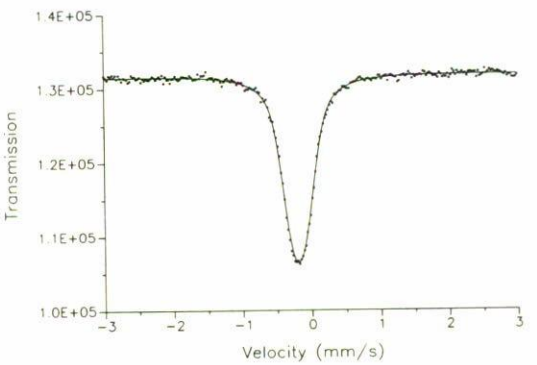

FIGURE 6. Fitting result with Eq. (18), calculated for $n = 8$ terms, for the spectrum of stainless steel foil, with a thickness of 8.5 mg/cm^2.

$f_a = 0.311$. For the stainless steel, with σ_0 modified by the factor: (natural width)/$(2w_a) = 0.587$, the $f_a = 0.65$ obtained is in agreement with the value obtained by Margulies *et al.* [6]. The fraction k for potassium ferrocyanide ($k = 0.603$) shows a Lorentzian component greater than the Gaussian component, and vice versa for stainless steel foil ($k = 0.367$). Therefore, due to the k value obtained both samples present a strong inhomogeneous broadening.

4. Conclusions

In this work an expression for the inhomogeneous broadening Mössbauer line-shape has been derived, including the TI as a particular case. This approximation is new because it considers the whole Mössbauer line-shape, and it is valid for thickness absorbers with different Lorentzian source and Lorentzian- Gaussian absorber widths. With this method it is possible to calculate the Lorentzian and Gaussian mixture through the k parameter.

1. F.J. Lynch, R.E. Holland, and M. Hamermesh, *Phys. Rev.* **120** (1960) 513.
2. D.A. Shirley, M. Kaplan, and P. Axel, *Phys. Rev.* **123** (1961) 816.
3. K.S. Singwi and A. Sjolander, *Phys. Rev.* **120** (1960) 1093.
4. H. Frauenfelder, *The Mössbauer effect*, (Benjamin, New York, 1963), p. 45.
5. S. Margulies and J. Ehrman, *Nucl. Instrum. Meth.* **12** (1961) 131.
6. S. Margulies, P. Debrunner, and H. Frauenfelder, *Nucl. Instrum. Meth.* **21** (1963) 217.
7. G. Lang, *Nucl. Instrum. Meth.* **24** (1963) 425.
8. G.A. Bykov and P.Z. Hien, *Z. Phys.* **43** (1962) 906; *Sov. Phys. JEPT* **16** (1963) 646.
9. E. Kankeleit, F. Boehm, and R. Hager, *Phys. Rev.* **134** (1964) B747.
10. W. Kündig, *Nucl. Instrum. Meth.* **48** (1967) 219.
11. J. Heberle, *Nucl. Instrum. Meth.* **58** (1968) 90.

12. M. Blume and J.A. Tjon, *Phys. Rev.* **165** (1968) 446.
13. D.J. Erickson and L.D. Roberts, *Phys Rev. B* **3** (1971) 2180.
14. B.T. Cleveland and J. Heberle, *Phys. Lett. A* **40** (1972) 13.
15. J. Stone, *Nucl. Instrum. Methods* **107** (1973) 285.
16. S. Mørup and E. Both, *Nucl. Instrum. Methods* **124** (1975) 445.
17. J.M. Williams and J.S. Brooks, *Nucl. Instrum. Methods* **128** (1975) 363.
18. P.J. Blamey, *Nucl. Instrum. Methods* **142** (1977) 553.
19. G.K. Shenoy, F.E. Wagner, and G.M. Kalvius, in *Mössbauer Isomer Shifts*, edited by G.K. Shenoy and F.E. Wagner (North-Holland Publishing Company, Netherlands, 1978), p. 97.
20. J. Friedt and J. Danon in *Modern Physics in Chemistry*, edited by E. Fluck and V.I. Goldanskii, Vol. 2 (Academic Press, New York, 1979), p. 209.
21. G. Longworth, in *Mössbauer Spectroscopy Applied to Inorganic Chemistry*, edited by G.J. Long, Vol. 1, (Plenum, New York, 1984), p. 49.
22. P. Jernberg, *Nucl. Instrum. Methods* **B4** (1984) 412.
23. J.G. Mullen *et al.*, *Phys. Rev. B* **37** (1988) 3226.
24. T.W. Guettinger and D.L. Williamson, *Nucl. Instrum. Methods* **B42** (1989) 268.
25. D.G. Rancourt, *Nucl. Instrum. Methods* **B44** (1989) 199.
26. H. Flores-Llamas, *Nucl. Instrum. Methods* **B94** (1994) 485.
27. B.R. Bullard, J.G. Mullen, and G. Schupp, *Phys Rev. B* **43** (1991) 7405.
28. B. Window, *J. Phys. E* **4** (1971) 401.
29. C.L. Chien, *Phys. Rev. B* **18** (1978) 1003.
30. G. Le Caer and J.M. Dubois, *J. Phys. E* **12** (1979) 1083.
31. G. Le Caer *et al.*, *Nucl. Instrum. Methods* **B5** (1984) 25.
32. D.G. Rancourt and J.Y. Ping, *Nucl. Instrum. Methods* **B58** (1991) 85.
33. D.A. O'Connor and G. Skyrme, *Nucl. Instrum. Methods* **106** (1973) 77.
34. T. Kobayashi and K. Fukumura, *Nucl. Instrum. Methods* **180** (1981) 549.
35. D.W. Posener, *Aust. J. Phys.* **12** (1959) 184.
36. M.J. Evans and P.J. Black, *J. Phys. C* **3** (1970) L81; *J. Phys. C* **3** (1970) 2167.
37. D.J. Erickson, J.F. Prince, and L.D. Roberts, *Phys Rev. C* **8** (1973) 1916.
38. H.C. Goldwire and J.P. Hannon, *Phys. Rev. B* **16** (1977) 1875.
39. B.R. Davis, S.E. Koonin, and P. Vogel, *Phys. Rev. C* **22** (1980) 1233.
40. M. Avery Snyder, *Chebyshev Methods in Numerical Approximation*, (Prentice-Hall, New Jersey, 1966), p. 45.
41. Y.L. Luke. *The Special Functions and their Approximations*, Vol. 2, (Academic Press, New York, 1969), p. 313.
42. G. Elste, *Z. Astrophys.* **33** (1953) 39.
43. P. Heinzel, *Bull. Astron. Inst. Czechosl.* **29** (1978) 159.
44. F.W.J. Olver, in *Handbook of Mathematical Functions*, edited by M. Abramowitz and L.A. Stegun, (Dover, New York, 1972), p. 375.
45. W. Gautschi, *SIAM J. Numer. Anal.* **7** (1970) 187.
46. W. Gautschi, in *Handbook of Mathematical Functions*, edited by M. Abramowitz and L.A. Stegun, (Dover, New York, 1972), p. 302.
47. J.J. Peyre and G. Principi, *Nucl. Instrum. Methods* **101** (1972) 605.
48. G.K. Wertheim, M.A. Butler, K.W. West, and D.N.E. Buchanan, *Rev. Sci. Instrum.* **45** (1974) 1369.
49. According to the manufacturer: The Radiochemical Center, little Chalfont, Amersham, England.
50. H. Flores-Llamas, H. Yee-madeira, G. Contreras-Puente, and R. Zamorano-Ulloa, *Hyp. Int.* **67** (1991) 711.
51. J. Hall and S.J. Lyle, *Nucl. Instrum. Methods* **163** (1979) 177.